Robust Hybrid Analog/Digital Beamforming for Uplink Massive-MIMO with Imperfect CSI

Alireza Morsali
Department of Electrical and
Computer Engineering, McGill University
Montreal, Canada
Email: alireza.morsali@mail.mcgill.ca

Benoit Champagne
Department of Electrical and
Computer Engineering, McGill University
Montreal, Canada
Email: benoit.champagne@mcgill.ca

***Abstract*—In this paper, we study the design of hybrid analog/digital beamformers for uplink connection in massive multiple-input multiple-output (MIMO) systems under imperfect channel state information (CSI). The norm-bounded channel error model is used to capture characteristics of imperfect CSI in practical systems. The objective function is formulated based on the minimum mean squared error (MMSE) worst-case robustness. We consider both single user (SU) and multiuser (MU) reception modes of a millimeter-Wave (mmWave) massive-MIMO base station (BS). For the SU scenario, we study hierarchical beamformer optimization as well as joint precoder/combiner optimization for users with limited and extended computational capabilities, respectively. These optimization techniques are subsequently extended to the MU case where a new hybrid robust combiner design is proposed. Simulation results are presented confirming the superiority of our designs when compared to recent robust hybrid designs in the literature.**

***Index Terms*—Hybrid beamforming, hybrid analog digital beamforming, massive-MIMO, mmWave, uplink, imperfect CSI.**

I. Introduction

Deployment of multiple antennas at both transmitter and receiver, i.e., multiple-input-multiple-output (MIMO) was undoubtedly a huge step up for wireless communication systems. While bandwidth is limited and increasing signal-to-noise ratio (SNR) only logarithmically increases the capacity, it has been shown that MIMO can linearly increase the capacity by increasing the number of antennas [1]. However, this is only true if the channel matrix is full rank which is not always the case, especially in millimeter wave (mmWave) systems [2], [3]. However, since in massive-MIMO the number of antennas can be very large, asymptotical limits of random matrix theory do apply and from an information-theoretic point of view, it follows that regardless of the channel characteristics, capacity increases linearly with the minimum number of antennas employed at either the transmitter or the receiver [4].

Nevertheless, the practical implementation of mmWave massive-MIMO systems faces many technical difficulties, and to this day remains very challenging and costly. In particular, since each antenna element must be driven by a radio frequency (RF) chain, the conventional implementation of massive-MIMO requires as many RF chains as the number of antenna elements. Even if the design and implementation of a MIMO system with such large number of RF chains was possible and worth the cost, the power consumption of such large number of RF components would seriously limit its potentials for application [5].

One the most effective solutions to this problem is hybrid analog and digital beamforming (HADB) [5]–[10]. In conventional fully digital (FD) systems, signal processing is performed in the digital domain by means of dedicated processors and/or digital circuitry, which requires each antenna to be connected to a dedicated RF chain. Consequently, the received signal of each antenna is available in the digital domain [11]–[13]. In HADB, another layer of analog signal processing is incorporated to the system and by doing so, it becomes possible to reduce the number of RF chains [5].

Various powerful MIMO techniques have been developed to date of which many are standardized and regularly being used in wireless systems [14]–[16]. Due to the special characteristics of mmWave channels, however, beamforming is the predominant MIMO technique. The HADB has an intricate structure where the entries of the RF precoder matrix must satisfy constant modulus constraint (i.e., phase-shifters).

In [6], a single RF chain scheme is proposed for realizing any given FD precoding. Since the ensuing precoder optimization is non-convex, many works have alternatively focused on designing HADB directly using heuristic iterative algorithms or reconstruction algorithms [7]–[10]. Specifically, in [9] and [10], robust hybrid combiner design for single user (SU) and multi-user (MU) are presented, respectively.

In this paper, we investigate the design of hybrid analog/digital beamformers for uplink connection in massive-MIMO systems under imperfect channel state information (CSI) for both single user (SU) and multi-user (MU) scenarios. The norm-bounded channel error model is used to represent the imperfect CSI aspects of practical systems and worst-case robustness minimum mean squared error (MMSE) is selected as the criterion to formulate the optimization problem. In the SU scenario, we consider the computational capabilities of the user for designing the beamformer. For users with limited computational resources, hierarchical optimization is presented which only puts the burden of robust calculations on

This work was supported by the Natural Sciences and Engineering Research Council of Canada (NSERC) and InterDigital Canada.

978-1-5386-7646-2/19/$31.00 ©2019 IEEE

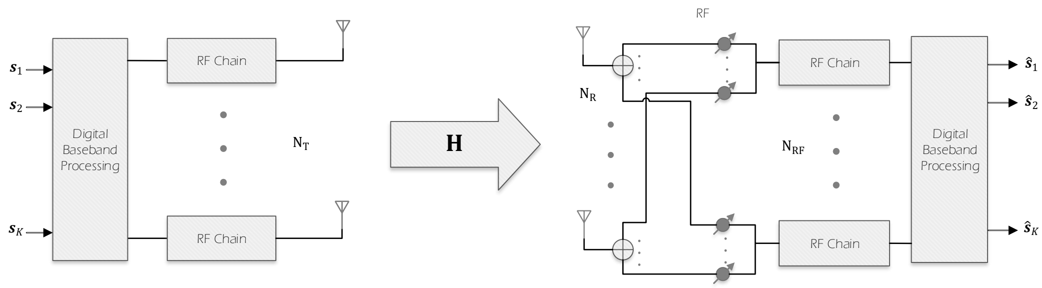

Fig. 1: Single user massive-MIMO system.

the base station (BS). For users with extended computational capabilities, joint precoder/combiner design is proposed. We then extend these optimization techniques to propose a new robust hybrid combiner design for MU. Simulation results are presented confirming the superiority of our design compared to recently published robust hybrid designs in the literature.

The paper is organized as follows. In Section II, the system model is explained. We then present our robust hybrid designs for the SU scenario in Section III followed by the MU hybrid combiner design in Section IV. Simulation results and conclusion are presented in Sections V ans VI, respectively.

Notations: Throughout this paper we use bold capital and lowercase letters to represent matrices and vectors, respectively. Superscripts $(.)^H$, $(.)^t$, and $(.)^*$ indicate Hermitian, transpose, and complex conjugations, respectively. $\mathbb{C}$ stands for complex field and $\mathbf{I}_n$ denotes an identity matrix of size $n \times n$. $\mathbf{A} = \text{diag}(a_1, a_2, \ldots, a_n)$ represents a diagonal matrix, in which $a_1, a_2, \ldots, a_n$ are placed diagonally on the matrix $\mathbf{A}$. A complex $n \times 1$ Gaussian random vector $\mathbf{x}$ with mean vector $\mathbf{m} = \mathbb{E}\{\mathbf{x}\}$ and covariance matrix $\mathbf{R} = \mathbb{E}\{\mathbf{x}^H \mathbf{x}\}$ is denoted by $\mathscr{CN}(\mathbf{m}, \mathbf{R})$.

II. System Model

We consider the uplink connection of a single-cell wireless system where the massive-MIMO BS has N_R receive antennas and N_{RF} RF chains with $N_{RF} \ll N_R$. In what follows, the system formulations of both SU and MU for uplink connection are presented.

A. SU System Model

For the SU scenario, we consider the general point-to-point MIMO system where the transmitter is considered to be a multiple-antenna user equipment (UE). As illustrated in Fig. 1, the UE is equipped with N_T antennas and the same number RF chains. The received signal at the BS can be written as:

$$\mathbf{y}_{\text{su}} = \mathbf{H}_{\text{su}} \mathbf{P} \mathbf{s} + \mathbf{n}, \tag{1}$$

where $\mathbf{H}_{\text{su}} \in \mathbb{C}^{N_R \times N_T}$ is the point-to-point mmWave MIMO channel matrix, $\mathbf{P} \in \mathbb{C}^{N_T \times K}$ and $\mathbf{s} \in \mathscr{A}^K$ are the precoder matrix and information symbol vector, respectively, where $\mathscr{A}$ is the selected constellation such as PSK or QAM and K is the number of transmitted symbols. Moreover, $\mathbf{n} \sim \mathscr{CN}(\mathbf{0}, \sigma^2 \mathbf{I}_{N_R})$ is the additive white Gaussian noise (AWGN) vector.

We consider the following well-known channel model for mmWave massive-MIMO with sparse scattering environments [6], [9]:

$$\mathbf{H} = \sqrt{\frac{N_T N_R}{L}} \sum_{l=1}^{L} \alpha^l \mathbf{a}_r(\phi_r^l) \mathbf{a}_t(\phi_t^l)^H, \tag{2}$$

where, $\alpha^l \sim CN(0,1)$ is the complex gain of l^{th} path, $\mathbf{a}_r$ and $\mathbf{a}_t$ are the antenna array responses of receiver and transmitter, respectively. ϕ_r^l and ϕ_t^l are arrival and departure angles and have uniform distribution over $[0, 2\pi)$. Moreover, $\mathbf{a}_r(\phi)$ and $\mathbf{a}_t(\phi)$ are the receiver and transmitter array responses. For uniform linear configuration, the array response is given by:

$$\mathbf{a}(\phi) = \frac{1}{\sqrt{N_R}} [1, e^{jkd \sin(\phi)}, ..., e^{jkd(N_R - 1)\sin(\phi)}], \tag{3}$$

where $k = 2\pi/\lambda$, and for wavelength of λ we have $d = \lambda/2$.

B. MU System Model

Without loss of generality, we assume K single antenna users are served by the BS as depicted in Fig. 2. The combined received signal from all K users with statistical channel inversion power control scheme [10] can be written as:

$$\mathbf{y}_{\text{mu}} = \mathbf{H}_{\text{mu}} \mathbf{s} + \mathbf{n}, \tag{4}$$

where $\mathbf{H}_{\text{mu}} \in \mathbb{C}^{N_R \times K}$ can be expressed as:

$$\mathbf{H}_{\text{mu}} = [\mathbf{h}_1, \mathbf{h}_2, ..., \mathbf{h}_K], \tag{5}$$

with $\mathbf{h}_k$ being the the uplink fading channel between kth user and BS. Moreover, $\mathbf{s} = [s_1, s_2, ..., s_K]^T$ is the symbol vector where $\mathbf{s}_i$ denotes the transmitted symbol of ith user. The mmWave channel vector of k^{th} user can be modeled as:

$$\mathbf{h}_k = \sqrt{\frac{N_R}{L_K}} \sum_{l=1}^{L_k} \alpha^{k,l} \mathbf{a}_r(\phi^l), \tag{6}$$

where $\alpha^{k,l} \sim CN(0, p_{k,l})$ is the complex gain of l^{th} path and:

$$\frac{1}{L_k} \sum_{l=1}^{k} p_{k,l} = 1, \tag{7}$$

for normalization purposes.

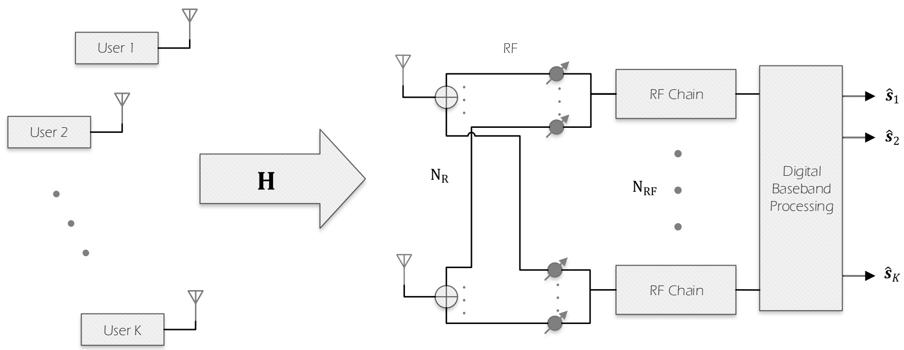

Fig. 2: Multi-user massive-MIMO system.

C. Hybrid Decoding

For $\mathbf{H}_i$ where $i = \{\text{su}, \text{mu}\}$, the total equivalent channel at the BS can be defined as:

$$\mathbf{H}_i^{eq} \triangleq \begin{cases} \mathbf{H}_{\text{su}}\mathbf{P} & i = \text{su} \\ \mathbf{H}_{\text{mu}} & i = \text{mu} \end{cases}. \tag{8}$$

We can thus formulate the decoded symbol vector for both cases after hybrid processing as:

$$\hat{\mathbf{s}} = (\mathbf{D_A D_D})^H \mathbf{H}_i \mathbf{s} + \mathbf{n_e}, \tag{9}$$

where, $\mathbf{n_e} = \mathbf{D_D}^H \mathbf{D_A}^H \mathbf{n}$ is the effective noise vector after linear combining. Matrices $\mathbf{D_D} \in \mathbb{C}^{N_{RF} \times K}$ and $\mathbf{D_A} \in \mathbb{U}^{N_R \times N_{RF}}$ are digital and analog combiners where:

$$\mathbb{U} = \{z \in \mathbb{C} \colon |z| = 1\}. \tag{10}$$

Analog combiner is implemented by RF phase shifters; therefore, all the entries of matrix $\mathbf{D_A}$ are constrained to have the same magnitude. For convenience, let us assume all analog matrices and vectors have unit magnitude entries, further practical discussions can be found in [6].

Finally, assuming $E\{\mathbf{s}\mathbf{s}^H\} = \mathbf{I}$, MSE between transmitted and decoded signals is the given by:

$$\text{MSE} \triangleq E\{\|\hat{\mathbf{s}} - \mathbf{s}\|^2\} \tag{11a}$$

$$= \|(\mathbf{D_A D_D})^H \mathbf{H}_i^{eq} - \mathbf{I}\|_F^2 + \sigma^2 \|\mathbf{D_A D_D}\|_F^2. \tag{11b}$$

D. Imperfect CSI

To represent the imperfect CSI characteristics of a practical system, the actual channel $\mathbf{H}_i$ can be expressed as:

$$\mathbf{H}_i = \hat{\mathbf{H}}_i + \boldsymbol{\Delta}, \tag{12}$$

where $\hat{\mathbf{H}}_i$ is the nominal channel known by the transceiver and $\boldsymbol{\Delta}$ is the error between the actual channel and the nominal channel which lies in an uncertainty region of $\mathscr{E}$:

$$\mathscr{E} \triangleq \{\boldsymbol{\Delta} : \|\boldsymbol{\Delta}\|_F \leq \varepsilon\}. \tag{13}$$

III. Hybrid Analog/Digital beamforming for SU massive-MIMO

We formulate the beamforming design problem based on the philosophy of worst-case robustness. The robust beamformer for SU can be obtained by solving the following optimization problem where P_T is the total power budget at the transmitter,

$$\min_{\mathbf{D_A}, \mathbf{D_D}, \mathbf{P}} \max_{\boldsymbol{\Delta} \in \mathscr{E}} \|(\mathbf{D_A D_D})^H (\hat{\mathbf{H}}_{su} + \boldsymbol{\Delta})\mathbf{P} - \mathbf{I}\|_F^2 + \sigma^2 \|\mathbf{D_A D_D}\|_F^2 \tag{14a}$$

$$\text{subject to} \quad \text{Tr}(\mathbf{P}\mathbf{P}^H) \leq P_T, \tag{14b}$$

$$\mathbf{D_A} \in \mathbb{U}^{N_R \times N_{RF}}. \tag{14c}$$

For designing the analog combiner, there are limitations in adjusting the magnitude of the combiner rows which is crucial in designing the robust combiner. Therefore, we design the analog combiner for the nominal channel and rely on the digital processing for robustness. Before designing the analog combiner, let us fix $N_{RF} = K$, as it is the minimum possible number of RF chains for decoding the received signal using linear operations [17]. Having the singular value decomposition of the nominal channel as:

$$\hat{\mathbf{H}}_{su} = \mathbf{U}_{su} \boldsymbol{\Sigma}_{su} \mathbf{V}_{su}^H. \tag{15}$$

The optimal fully digital combiner for eigen beam transmission is given by [18], [19]:

$$\mathbf{D} = \mathbf{U}_{su}^a, \tag{16}$$

where $\mathbf{U}_{su} = [\mathbf{U}_{su}^a, \mathbf{U}_{su}^b]$ and $\mathbf{U}_{su}^a$ contains the first K columns of $\mathbf{U}_{su}$. We now formulate the analog decoder design as:

$$\min_{\mathbf{D_A}} \quad \|\mathbf{D_A} - \mathbf{D}\|_F^2 \tag{17a}$$

$$\text{subject to} \quad \mathbf{D_A} \in \mathbb{U}^{N_R \times N_{RF}}, \tag{17b}$$

$$\mathbf{D_A}^H \mathbf{D_A} = \mathbf{I}_{N_{RF}}. \tag{17c}$$

Our intentions behind introducing the constraint (17c) are threefold: firstly, to avoid coloring the noise; secondly, maintaining the noise power, and thirdly, to avoid amplifying the channel error power after analog decoding. Since this problem is non-convex, we first relax the unit modulus constraint:

$$\hat{\mathbf{D}}_A^* = \min_{\mathbf{D_A}} \quad \|\hat{\mathbf{D}}_A - \mathbf{D}\|_F^2 \tag{18a}$$

$$\text{subject to} \quad \|\hat{\mathbf{D}}_A\|_F^2 \leq N_{RF}N_R, \tag{18b}$$

$$\hat{\mathbf{D}}_A^H\hat{\mathbf{D}}_A = \mathbf{I}_{N_{RF}}. \tag{18c}$$

Fortunately, the optimization problem (18) admits a closed form solution [20]:

$$\hat{\mathbf{D}}_A^* = \mathbf{D}(\mathbf{D}^H\mathbf{D})^{(1/2)}. \tag{19}$$

Using (19), we arrive at a solution for analog decoder by projecting $\hat{\mathbf{D}}_A^*$ on the ring $\mathbb{U}$:

$$\mathbf{D}_A = \text{proj}_{\mathbb{U}}(\hat{\mathbf{D}}_A^*), \tag{20}$$

where $\text{proj}_{\mathbb{U}}$ is the following element-wise operation on each entry of the given matrix:

$$e^{j\theta} = \text{proj}_{\mathbb{U}}(\alpha e^{j\theta}). \tag{21}$$

For simplicity, let us define the equivalent channel after analog combining as:

$$\hat{\mathbf{H}}_{su}^e \triangleq \mathbf{D_A}^H\hat{\mathbf{H}}_{su}. \tag{22}$$

Having designed the analog combiner, we can omit the constraint (14c) from the optimization problem (14). This problem however is required to be solved by both BS and UE to jointly optimize the precoder and combiner for worst-case robustness. Nevertheless, it is possible that the UE does not have enough computational power to perform the extra required computations. Therefore, we propose beamformer designs for both cases where the UE can and cannot perform the robustness calculations.

A. Hierarchical Robust Hybrid Beamformer Design

Here, we explore the case that the UE does not have enough computational resources to perform joint robust optimization. Thus, hierarchical optimization is performed to design beamformers. To do so, we first design the optimal precoding at UE for the equivalent nominal channel after analog combining i.e., $\hat{\mathbf{H}}_{su}^e$. Under the assumption that the receiver is capable of optimal decoding, we can decouple the transmitter and the receiver designs. Therefore, the precoder can be obtained by solving the following optimization problem [17]:

$$\max_{\mathbf{P}} \quad \log_2\left(\det(\mathbf{I}_K + \frac{1}{\sigma^2}\mathbf{R}_n^{-1}\hat{\mathbf{H}}_{su}^e\mathbf{P}\mathbf{P}^H\hat{\mathbf{H}}_{su}^e)\right) \tag{23a}$$

$$\text{subject to} \quad \text{Tr}(\mathbf{P}\mathbf{P}^H) \leq P_T, \tag{23b}$$

$$\mathbf{R}_n = \mathbf{D_A}^H\mathbf{D_A}. \tag{23c}$$

Since we have already designed analog combiner with the constraint (17c), for large N_R we have:

$$\mathbf{D_A}^H\mathbf{D_A} \approx \mathbf{I}_K. \tag{24}$$

Then, the optimal solution of (23) can be analytically calculated [21] using the singular value decomposition of $\hat{\mathbf{H}}_{su}^e$:

$$\hat{\mathbf{H}}_{su}^e = \mathbf{U}_{su}^e\mathbf{\Sigma}_{su}^e{\mathbf{V}_{su}^e}^H. \tag{25}$$

The optimal non-robust precoder is:

$$\mathbf{P}_{nr} = \mathbf{V}_{su}^e\mathbf{W}, \tag{26}$$

where the diagonal weight matrix $\mathbf{W}$ is calculated via water filling [21]. Now, we can rewrite the worst-case optimization problem as:

$$\min_{\mathbf{D_D}} \quad \max_{\mathbf{\Delta}\in\mathscr{E}} \quad \|\mathbf{D_D}^H(\hat{\mathbf{H}}_{su}^e + \mathbf{\Delta})\mathbf{P} - \mathbf{I}\|_F^2 + \sigma^2\|\mathbf{D_D}\|_F^2 \tag{27a}$$

$$\text{subject to} \quad \mathscr{E} = \{\mathbf{\Delta} : \|\mathbf{\Delta}\|_F \leq \varepsilon\|\mathbf{D_A}\|_F\}. \tag{27b}$$

Using Theorem 1 in [18], for the chosen precoder, the optimal solution of the above problem is given by:

$$\mathbf{D_D}^H = \mathbf{\Sigma}_D{\mathbf{U}_{su}^e}^H, \tag{28}$$

with $\mathbf{\Sigma}_D = \text{diag}\big([d_1, d_2, ..., d_K]\big)$ and d_i's are roots of the following equation:

$$\phi(d_i) = -\frac{2\mu w_i(d_i\gamma_i w_i - 1)(d_i w_i - \mu\gamma_i)}{(\mu - d_i^2 w_i^2)^2} + 2\sigma^2 d_i = 0 \tag{29}$$

where μ is an auxiliary variable which must be optimized as well, w_i's and γ_i's are diagonal entries of $\mathbf{W}$ and $\mathbf{\Sigma}_{su}^e$, respectively. Simple algorithmic solutions of (29) are given in [18].

B. Joint Robust Hybrid Precoder/Combiner Design

If the SU has enough computational power to perform the robust calculations, the worst-case beamformer design for the selected hybrid combiner (20) can be written as:

$$\min_{\mathbf{D_D},\mathbf{P}} \quad \max_{\mathbf{\Delta}\in\mathscr{E}} \quad \|\mathbf{D_D}^H(\hat{\mathbf{H}}_{su}^e + \mathbf{\Delta})\mathbf{P} - \mathbf{I}\|_F^2 + \sigma^2\|\mathbf{D_D}\|_F^2 \tag{30a}$$

$$\text{subject to} \quad \text{Tr}(\mathbf{P}\mathbf{P}^H) \leq P_T. \tag{30b}$$

This problem can be efficiently solved using alternating optimization techniques [5], [17], [18]. By fixing $\mathbf{P}$ in (30), we arrive at (27) which we have solved in previous subsection and by fixing $\mathbf{D_D}$ we can write:

$$\min_{\mathbf{P}} \quad \max_{\mathbf{\Delta}\in\mathscr{E}} \quad \|\mathbf{D_D}^H(\hat{\mathbf{H}}_{su}^e + \mathbf{\Delta})\mathbf{P} - \mathbf{I}\|_F^2 + \sigma^2\|\mathbf{D_D}^H\|_F^2 \tag{31a}$$

$$\text{subject to} \quad \text{Tr}(\mathbf{P}\mathbf{P}^H) \leq P_T. \tag{31b}$$

The optimal solution of (31) can be written as [19]:

$$\mathbf{P}_{rob} = \mathbf{V}_{su}^e\text{diag}(\mathbf{w}), \tag{32}$$

where $\mathbf{w} = [w_1, \ldots, w_K]^T$ and w_i's is the allocated power of ith symbol. Here, we present a suboptimal solution with low computational complexity which can be used in alternating joint optimization. Pursuing the same guideline we took to solve (27), we can first calculate $\hat{\mathbf{w}} = [\hat{w_1}, \ldots, \hat{w_K}]^T$ for the unconstrained optimization (31a), where $\hat{w}_1$'s are the roots of:

$$\psi(\hat{w}_i) = -\frac{2\mu\hat{w}_i(d_i\gamma_i\hat{w}_i - 1)(d_i\hat{w}_i - \mu\gamma_i)}{(\mu - d_i^2{\hat{w}_i}^2)^2} + 2\sigma^2 d_i = 0. \tag{33}$$

Algorithm 1 Joint Robust Precoder/Combiner Design

Given: $\mathbf{U}^e_{su}$, $\mathbf{V}^e_{su}{}^H$, P_T, $\varepsilon\|\mathbf{D_A}\|_F$
Initializing: $\mathbf{P} = \mathbf{V}^e_{su}$, $\mathbf{D_D}{}^H = \mathbf{U}^e_{su}{}^H$
1. $\mathbf{\Sigma}_D = \text{diag}([d_1, d_2, ..., d_K])$ where d_i's are roots of (29).
2. $\mathbf{D_D}{}^H = \mathbf{\Sigma}_D \mathbf{U}^e_{su}{}^H$.
3. Calculate $\mathbf{w}$ from (34).
4. $\mathbf{P} = \mathbf{V}^e_{su}\text{diag}(\mathbf{w})$.
5. Iterate until convergence .
Outputs: $\mathbf{P}_{rob} = \mathbf{P}$, $\mathbf{D_D}{}^H$.

Note that (33) can be solved in a similar fashion as (29). Then, to satisfy (31b), by defining $\rho = \sqrt{P_T}/\|\hat{\mathbf{w}}\|$, we have:

$$\mathbf{w} = \rho\hat{\mathbf{w}}. \tag{34}$$

We summarized our proposed joint robust transceiver design based on alternating optimization in algorithm 1. Note that, (34) is a simple low-complexity suboptimal power allocation. In [19], an algorithmic solution is presented to obtain optimal w_i's. Therefore, if the system can handle the required complicated computations, the optimal robust precoder/combiner design can obtained by changing line 3 of algorithm 1 to: "*3. Calculate* $\mathbf{w}$ *from Algorithm 1 in [19]* ".

IV. MU Hybrid Combiner Design

In this section, we explore robust combiner design for MU scenario by formulating the worst-case optimization as:

$$\min_{\mathbf{D_A},\mathbf{D_D}} \max_{\mathbf{\Delta}\in\mathscr{E}} \|(\mathbf{D_A}\mathbf{D_D})^H(\hat{\mathbf{H}}_{mu}+\mathbf{\Delta})-\mathbf{I}\|_F^2 + \sigma^2\|\mathbf{D_A}\mathbf{D_D}\|_F^2 \tag{35a}$$

$$\text{subject to} \quad \mathbf{D_A} \in \mathbb{U}^{N_R\times N_{RF}}. \tag{35b}$$

Comparing the above optimization with (14), one can observe that if we set $\mathbf{P} = \mathbf{I}_K$ in (14) we arrive at (35). Therefore, In order to solve the above optimization problem we can use the proposed solution in Section III by assuming $\mathbf{P} = \mathbf{I}_K$.

As a result, considering the singular value decomposition of the nominal MU channel:

$$\hat{\mathbf{H}}_{mu} = \mathbf{U}_{mu}\mathbf{\Sigma}_{mu}\mathbf{V}^H_{,u}, \tag{36}$$

the analog combiner is given as:

$$\mathbf{D}_A = \text{proj}_{\mathbb{U}}\big(\mathbf{D}(\mathbf{D}^H\mathbf{D})^{(1/2)}\big), \tag{37}$$

with

$$\mathbf{D} = \mathbf{U}^a_{mu}, \tag{38}$$

where $\mathbf{U}_{mu} = [\mathbf{U}^a_{mu}, \mathbf{U}^b_{mu}]$ i.e., $\mathbf{U}^a_{mu}$ contains the first K columns of $\mathbf{U}_{mu}$. Then, defining the equivalent channel after analog combining as:

$$\hat{\mathbf{H}}^e_{mu} \triangleq \mathbf{D_A}{}^H\hat{\mathbf{H}}_{mu}, \tag{39}$$

and having its singular value decomposition as:

$$\hat{\mathbf{H}}^e_{mu} = \mathbf{U}^e_{mu}\mathbf{\Sigma}^e_{mu}\mathbf{V}^e_{mu}{}^H. \tag{40}$$

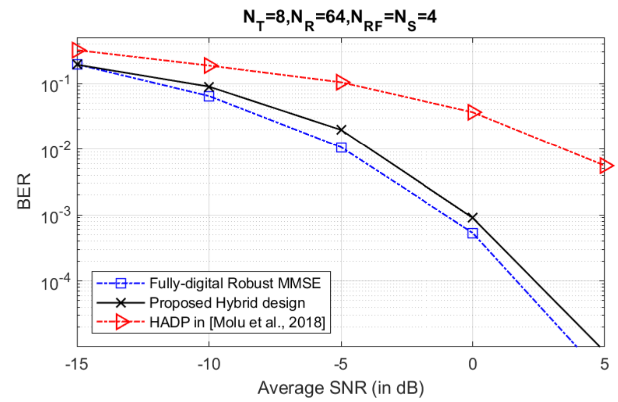

Fig. 3: BER versus SNR for [9], fully digital robust MMSE and our design in a 8×64 massive-MIMO system.

The digital combiner is then obtained from:

$$\mathbf{D_D}{}^H = \mathbf{\Sigma}_D\mathbf{U}^e_{mu}{}^H, \tag{41}$$

with $\mathbf{\Sigma}_D = \text{diag}([d_1, d_2, ..., d_K])$ and d_i's are roots of the following equation:

$$\phi(d_i) = -\frac{2\mu(d_i\gamma_i - 1)(d_i - \mu\gamma_i)}{(\mu - d_i^2)^2} + 2\sigma^2 d_i = 0, \tag{42}$$

where μ is an auxiliary variable, and γ_i's are diagonal entries of $\mathbf{\Sigma}^e_{su}$. The roots of (42) can be obtained in a similar fashion as (29).

V. Simulation Results

In this section, we present simulation results for both SU and MU cases. To obtain realistic results, we do not perform simulations only for the worst possible channel in the uncertainty region, instead the elements of the channel error $\mathbf{\Delta}$ are randomly generated according to zero-mean, i.i.d. Gaussian distributions such that $\|\mathbf{\Delta}\|_F = \varepsilon$. The radius of uncertainty region ε is calculated by $\varepsilon^2 = s\|\hat{\mathbf{H}}|_F^2$ where $s \in [0, 1)$. For all the simulations, number of receive antennas at the BS is set to $N_R = 64$ and the uniform linear configuration is used.

In SU scenario, 8-PSK constellation is used. For UE with $N_T = 8$ transmit antennas, $N_s = 4$ symbols per transmission, $s = 0.01$ and mmWave channel with $L = 10$ paths, Fig. 3 depicts the BER performance versus SNR (SNR=P_T/σ^2) for fully digital beamforming, our proposed hierarchical design in Section III-A, and hybrid robust design in [9]. While there is around less than 1 dB gap between our design and fully digital beamforming, our proposed design outperforms [9] by more than 6 dB.

Simulation results for the case where both BS and UE perform joint robust optimization are illustrated in Fig. 4. The UE is equipped with $N_T = 32$ transmit antennas, and the rest of parameters are set as follows: $N_s = 8$ symbols per transmission, $s = 0.03$ and mmWave channel with $L = 15$. The results expectedly confirm the superiority of our design to the recently published robust design [9].

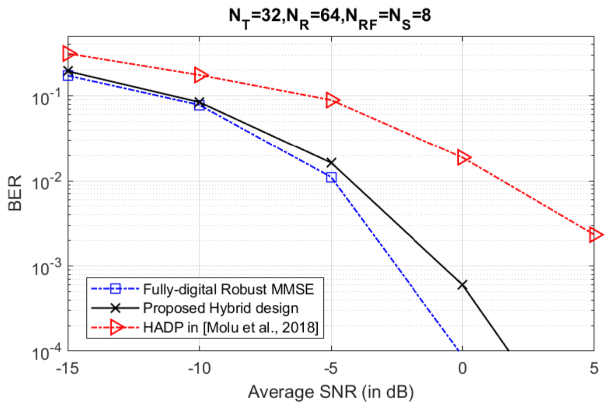

Fig. 4: BER versus SNR for [9], fully digital robust MMES and our design in a 32×64 massive-MIMO system.

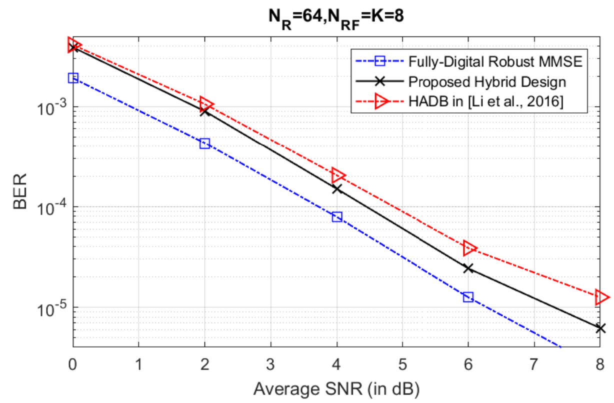

Fig. 5: BER versus SNR for [10], fully digital and our design in a 64 massive-MIMO system

For multi-user case, 16-QAM constellation and independent multipath channel model [10] is used. We compared our design with robust hybrid design in [10] as well as fully digital decoder as the benchmark. For $K = 8$ single antenna users, and independent mmWave channels with $L_k = 15$ with $s = 0.001$, Fig. 5 illustrates the BER performance versus SNR. It can be observed that our design has a margin of 1 dB to the fully digital combining and outperforms the robust design in [10] by more than 1 dB.

VI. Conclusion

In this paper, we proposed robust hybrid analog/digital bemformer designs for uplink in massive-MIMO communication systems. Both SU and MU reception modes in uplink direction of a single-cell configuration with massive-MIMO BS were considered. The norm-bounded channel error was used to capture the imperfect CSI conditions and the objective function was formulated based on the worst-case robustness MMSE. For SU scenario, we presented hierarchical optimization as well as joint optimization based on UE capabilities to perform extra calculations required for robust transceiver design. We then proposed robust hybrid combiner design for MU uplink connection. Finally, presented simulation results illustrated the superiority of our design to recently published hybrid designs.

References

[1] E. Telatar, “Capacity of multi-antenna gaussian channels,” *European Transactions on Telecommunications*, vol. 10, no. 6, pp. 585–595, 1999.

[2] S. A. Busari, K. M. S. Huq, S. Mumtaz, L. Dai, and J. Rodriguez, “Millimeter-Wave Massive MIMO Communication for Future Wireless Systems: A Survey,” *IEEE Communications Surveys Tutorials*, vol. PP, no. 99, pp. 1–1, 2017.

[3] R. C. Daniels and R. W. Heath, “60 ghz wireless communications: Emerging requirements and design recommendations,” *IEEE Trans. Veh. Technol.*, vol. 2, no. 3, pp. 41–50, Sept. 2007.

[4] E. G. Larsson, O. Edfors, F. Tufvesson, and T. L. Marzetta, “Massive mimo for next generation wireless systems,” *IEEE Commun. Mag.*, vol. 52, no. 2, pp. 186–195, Feb. 2014.

[5] A. Alkhateeb, J. Mo, N. Gonzalez-Prelcic, and R. W. Heath, “MIMO Precoding and Combining Solutions for Millimeter-Wave Systems,” *IEEE Commun. Mag.*, vol. 52, no. 12, pp. 122–131, Dec. 2014.

[6] A. Morsali, A. Haghighat, and B. Champagne, “Realizing Fully Digital Precoders in Hybrid A/D Architecture With Minimum Number of RF Chains,” *IEEE Commun. Lett.*, vol. 21, no. 10, pp. 2310–2313, Oct. 2017.

[7] F. Khalid, “Hybrid beamforming for millimeter wave massive multiuser mimo systems using regularized channel diagonalization,” *IEEE Commun. Lett.*, pp. 1–1, 2018.

[8] T. Lin, J. Cong, Y. Zhu, J. Zhang, and K. B. Letaief, “Hybrid beamforming for millimeter wave systems using the mmse criterion,” *IEEE Trans. Commun.*, pp. 1–1, 2019.

[9] M. M. Molu, P. Xiao, M. Khalily, K. Cumanan, L. Zhang, and R. Tafazolli, “Low-complexity and robust hybrid beamforming design for multi-antenna communication systems,” *IEEE Trans. Wireless Commun.*, vol. 17, no. 3, pp. 1445–1459, Mar. 2018.

[10] J. Li, L. Xiao, X. Xu, and S. Zhou, “Robust and low complexity hybrid beamforming for uplink multiuser mmwave MIMO systems,” *IEEE Commun. Lett.*, vol. 20, no. 6, pp. 1140–1143, June 2016.

[11] S. Tofigh, H. M. Kermani, and A. Morsali, “A new design criterion for linear receiver stbcs based on full-rank spaces,” *IEEE Commun. Lett.*, vol. 19, no. 2, pp. 207–210, Feb. 2015.

[12] M. Samavat, A. Morsali, and S. Talebi, “Delay interleaved cooperative relay networks,” *IEEE Commun. Lett.*, vol. 18, no. 12, pp. 2137–2140, Dec. 2014.

[13] A. Morsali and S. Talebi, “On permutation of space-time-frequency block codings,” *IET Commun.*, vol. 8, no. 3, pp. 315–323, Feb. 2014.

[14] M. Shahabinejad, A. Morsali, S. Talebi, and M. Shahabinejad, “On the coding advantages of the quasi-orthogonal space-frequency block codes,” *IET Commun.*, vol. 8, no. 4, pp. 525–529, Mar. 2014.

[15] F. Koroupi, A. Morsali, V. Niktab, M. Shahabinejad, and S. Talebi, “Quasi-orthogonal space-frequency and space-time-frequency block codes with modified performance and simplified decoder,” *IET Commun.*, vol. 11, no. 11, pp. 1655–1661, Sept. 2017.

[16] A. Morsali, S. Tofigh, Z. Mohammadian, and S. Talebi, “Coding advantage decomposition inequality for the space-frequency block codes,” *IET Commun.*, vol. 8, no. 4, pp. 500–507, Mar. 2014.

[17] F. Sohrabi and W. Yu, “Hybrid digital and analog beamforming design for large-scale antenna arrays,” *IEEE J. Sel. Topics Signal Process.*, vol. 10, no. 3, pp. 501–513, Apr. 2016.

[18] J. Wang and M. Bengtsson, “Joint Optimization of the Worst-Case Robust MMSE MIMO Transceiver,” *IEEE Signal Processing Lett.*, vol. 18, no. 5, pp. 295–298, May 2011.

[19] J. Wang and D. P. Palomar, “Robust MMSE Precoding in MIMO Channels With Pre-Fixed Receivers,” *IEEE Trans. Signal Processing*, vol. 58, no. 11, pp. 5802–5818, Nov. 2010.

[20] Y. C. Eldar, “Least-squares inner product shaping,” *Linear Algebra and its Applications*, vol. 348, no. 1, pp. 153–174, 2002.

[21] E. Torkildson, U. Madhow, and M. Rodwell, “Indoor millimeter wave mimo: Feasibility and performance,” *IEEE Trans. Wireless Commun.*, vol. 10, no. 12, pp. 4150–4160, Dec. 2011.